**Summary:** We explored the diffusion mechanisms in a series of liquid/glassy polymer interphases. The diffusion experiments were performed in a unique way: the temperature range studied encompassed the glass transition temperature ($T_g$) of the glassy matrices. We observed that the diffusion behavior of the liquid polymer was remarkably continuous when passing through the matrix $T_g$, and that the diffusion modes at the liquid/glassy interphases were very similar to those observed in liquid/liquid polymer diffusion.

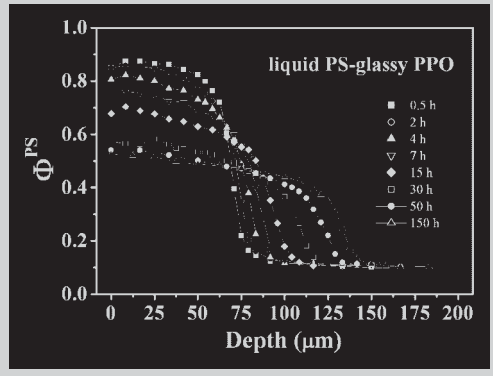


Diffusion profiles of liquid PS in glassy PPO obtained by confocal Raman spectroscopy. The sample was held at 160 °C for the times indicated in the plot.

# Diffusion Kinetics at Liquid-Glassy Polymer Interphases

*Luis Arzondo,*[1] *J. Pablo Tomba,**[1,a] *José M. Carella,*[1] *José M. Pastor*[2]

[1] Institute of Materials Science and Technology (INTEMA), National Research Council (CONICET), University of Mar del Plata, Juan B. Justo 4302, 7600 Mar del Plata, Argentina
E-mail: jptomba@fi.mdp.edu.ar
[2] Department of Physics of Condensed Matter, University of Valladolid, Paseo del Cauce s/n 47011 Valladolid, Spain

Received: December 20, 2004; Revised: February 26, 2005; Accepted: March 1, 2005; DOI: 10.1002/marc.200400643

**Keywords:** Case-II diffusion; confocal Raman microspectroscopy; glassy polymer matrices; polymer diffusion

## Introduction

Diffusion of organic liquids in contact with amorphous glassy polymer matrices has been a topic of long standing interest in polymer physics. The process plays an important role in both the manufacture and final properties of many polymer-based products. Some remarkable examples are lithography in microelectronics, polymers for barrier applications, polymer blends and alloys with hard and soft components, and drug delivery systems, among many others.

For a long time, diffusion at glassy polymer matrices was synonymous with the penetration of small molecules, mostly investigated by sorption techniques.[1] Under certain conditions, small sized molecules, particularly those that swell glassy polymers, can diffuse and penetrate into polymer matrices following the Case-II diffusion mechanism. Thomas and Windle[1] established the main characteristics and the rate-controlling step of this remarkable non-Fickean diffusion process, confirmed later by Kramer and coworkers.[2,3] The penetration of the small molecules causes an osmotic pressure-driven deformation process,[1] where the glassy polymer outer layers act as semi-permeable membranes through which the small size molecules can diffuse. Case-II diffusion is established when the stress caused by the osmotic-driven penetration of small molecules overcomes the yield stress of the glassy matrix.[3] At this point, the diffusion process is controlled by the time-dependent mechanical response of the polymer to the osmotic swelling stress at the penetrant diffusion front, which constitutes the central aspect of Case-II.[1] As a consequence, sorption kinetics and diffusion front advances in Case-II conditions vary linearly with time, in marked contrast with the square root of time scaling that generally characterizes the Fickean diffusion.

On the contrary, diffusion of large molecules, i.e., polymers in the liquid state, in glassy polymer matrices has been a less studied case. Results have been reported only for miscible polymers pairs, where the Flory-Huggins

[a] Present address: Department of Chemistry, University of Toronto, 80 St. George Street, Toronto, Canada M5S 3H6
E-mail: jptomba@chem.utoronto.ca.

 

thermodynamic interaction parameter is favorable.[4–9] The diffusion mechanisms in these systems are still under discussion and have been a subject of controversy. Some authors have extended the concept of Case-II to explain the diffusion mechanism at the liquid/glassy polymer interphase, claiming that the process is controlled by the mechanical response of the glassy polymer.[5–7] This idea has been predominant in many papers published about this topic, including some very recent ones.[10] Other authors have questioned this view pointing out that large molecules, such as liquid polymers, are associated with extremely low osmotic pressures, insufficient to trigger a mechanism of mechanically controlled penetration.[9] These authors have suggested that in these cases the interphase evolution is diffusion controlled, as observed in liquid-liquid diffusion between polymers with different physical properties.[9,11]

We started this project with the objective of discerning between these different views about the mechanisms that control the interfacial growth in liquid/glassy polymer blends. We focused our investigation on two miscible polymer pairs: a) liquid poly(vinyl methyl ether)-glassy polystyrene (*l*-PVME/PS); and b) liquid PS-glassy poly-(phenylene oxide) (*l*-PS/PPO). For these systems, the diffusion mechanisms reported in the literature are contradictory,[9,10] or based on studies not systematic enough to be convincing.[5,6,10] We also wanted to investigate whether the observed mechanism is a general or a particular one (e.g., osmotic pressure effects are only dependent on molecular sizes). We studied planar *l*-PVME/PS and *l*-PS/PPO interphases by ''optical sectioning'' with confocal Raman microspectroscopy, a technique that allows direct observation of the chemical composition profiles at the interphase. The strategy we followed consisted of performing the diffusion experiments in temperature ranges that encompassed the glass transition temperatures ($T_g$) of the glassy matrices, with the specific purpose of directly comparing diffusion rates for liquid-liquid and liquid-solid polymer diffusion in the same polymer pair and using the same experimental technique. This communication reports on our preliminary results, which show that in both polymer pairs the diffusion process presents the same features, independent of the physical state of the matrix.

## Experimental Part

PS (referred to as PS227, $\overline{M}_w = 227\,000$ g · mol$^{-1}$, $\overline{M}_w/\overline{M}_n = 1.05$, $T_g = 102$ °C) and PVME ($\overline{M}_n = 4\,000$ g · mol$^{-1}$, $\overline{M}_w/\overline{M}_n = 1.05$, $T_g = -33$ °C) used for the *l*-PVME/PS experiments were purchased from Polymer Source (Dorval, Canada). Experiments involving the *l*-PS/PPO polymer pair were carried out using two anionically synthesized PS from Polymer Source. These samples are referred to here as PS1.5 ($\overline{M}_w = 1\,460$ g · mol$^{-1}$, $T_g = 45$ °C) and PS3.9 ($\overline{M}_w = 3\,900$ g · mol$^{-1}$, $T_g = 77$ °C); $\overline{M}_w/\overline{M}_n < 1.1$ in both samples. The PPO sample was purchased from Aldrich ($\overline{M}_w = 31\,000$ g · mol$^{-1}$, $\overline{M}_w/\overline{M}_n = 2.0$, $T_g = 212$ °C). The $T_g$ for the pure polymers and blends were measured by differential scanning calorimetry, with a Perkin-Elmer Pyris II DSC instrument, at a heating rate of 10 °C · min$^{-1}$. The molecular-weight characterization was provided by the manufacturers.

The bi-layered samples used for diffusion experiments are described in Table 1. Polymer blends for the bi-layers were prepared by freeze-drying benzene solutions at 10% (w/w). Antioxidant (200 ppm, Santonox, Ciba-Geigy) was added to the blends to prevent degradation. Polymer bi-layers, in the form of cylindrical specimens (20 mm diameter), were prepared by sequential vacuum molding of a thin low-$T_g$ layer (40–150 μm thick) on top of a thicker high-$T_g$ layer (500 μm thick), as explained elsewhere.[12] For details about the compositions of the layers see Table 1. Diffusion between polymer layers was promoted by annealing in a temperature-controlled oven (±0.5 °C) for specified times. The oven was continuously flushed with dry nitrogen to avoid oxidation of the samples. We kept the liquid-solid interphase strictly horizontal at all times, to prevent the flow of the low-viscosity thin layer. The samples were periodically removed from the oven and were allowed to quickly cool back to room temperature, which virtually stops polymer diffusion, before Raman measurements were performed.

Local Raman spectra were measured at room temperature, on a Raman microspectrometer DILOR LabRam Confocal, equipped with a 16 mW He-Ne laser beam (632.8 nm wavelength). A slit opening of 500 μm and a holographic grating of 1 800 lines · mm$^{-1}$ were used (spectral resolution of 5 cm$^{-1}$). The technique was employed in the depth-profiling mode. We used an Olympus 100× objective (NA = 0.9) in combination with pinhole openings between 100–300 μm (the maximum aperture is 1 000 μm), which renders a nominal depth resolution of 4 μm. As explained in earlier work,[13] the resolution for

Table 1. Characteristics of the samples used in the diffusion experiments. PS227, PS3.9, and PS1.5 identify PS with an $\overline{M}_w$ of 227 000, 3 900, and 1 460 g · mol$^{-1}$ respectively. $\Phi^{liq}$ refers to the initial volume fraction of the low-$T_g$ component in each of the layers. Thickness refers to the range of initial thickness of the low-$T_g$ layer examined in our experiments (not all of them were shown here). The high-$T_g$ layer is about 500 μm thick.

| System | Low-$T_g$ layer | | | High-$T_g$ layer | | Diffusion temperatures |
|---|---|---|---|---|---|---|
| | $\Phi^{liq}$ | $T_g$ | Thickness | $\Phi^{liq}$ | $T_g$ | °C |
| | | °C | μm | | °C | |
| *l*-PVME/PS227 | 0.8 | −30 | 60–75 | 0.0 | 100 | 85, 105, 125 |
| *l*-PS1.5/PPO | 0.9 | 51 | 40–70 | 0.1 | 182 | 140, 160, 180, 200 |
| *l*-PS3.9/PPO | 0.9 | 80 | 70–125 | 0.1 | 185 | 160, 180, 200, 220 |

depth-profiling decreases progressively as a function of depth. Concentration profiles for each diffusion time were measured by taking several Raman spectra from different depths along the diffusion path in steps of 2–5 μm (typically 30–40 points). The acquisition time for each spectrum was 30 s and 8 spectra were accumulated for each data point. The acquired Raman spectra were translated to local chemical compositions with the linear decomposition method.[14] The procedure was repeated for several diffusion times, always focusing the laser beam within 10 μm of the same spot at the sample surface.

## Results and Discussion

Figure 1 shows representative liquid PS concentration profiles obtained from diffusion experiments in the *l*-PS/PPO polymer pair. To obtain these profiles, confocal Raman ''optical sectioning'' was started at the outer PS surface, the zero in the depth scale axis, and then repeated at deeper positions along the PS diffusion path. We examined a range of temperatures that encompasses the $T_g$ of the glassy matrix, a PPO-rich blend in this case. The top panel in Figure 1 shows PS3.9 concentration profiles corresponding to a sample annealed at 200 °C, which is 15 °C above the $T_g$ of the PPO-rich matrix, for several diffusion times. The bottom panel shows PS1.5 concentration profiles for a sample annealed at 160 °C, which is 23 °C below the $T_g$ of the PPO-rich matrix.

The liquid PS concentration profiles shown in Figure 1 are markedly asymmetric. They are characterized by a fairly flat region along the outer first 50–75 μm, where the PS concentration is uniform. Note that because of the limited PS supply, the concentration of liquid polymer throughout this region decreases with diffusion time.[12] The profile slope then becomes increasingly higher and the PS concentration rapidly decreases, until the depths of the pure matrix are reached. The transition region between the PS-rich and PPO-rich layers appears artificially smoothed because of limitations in the spatial resolution of the confocal Raman technique. In the depth-profiling mode, the spatial resolution decreases as we focus the laser beam deeper into the sample; for this reason, the broadening is more pronounced in those interphases located at higher depths. This problem has been thoroughly analyzed and quantified in previous work.[12,13] We have shown that the actual transition between the low- and high-$T_g$ layers is abrupt and occurs in a narrow range on the depth scale (1–2 μm), as determined by using a focusing mode with invariant and superior instrumental resolution (surface profiling, 1.5 μm resolution).[13] Hence, these liquid PS concentration profiles, which can be thought as having a ''plateau'' region with uniform liquid polymer concentration followed by a sharply defined drop in concentration or ''diffusion front'', advance into the glassy (or highly viscous) matrix maintaining an almost rectangular-box shape. The same features described above also characterize the liquid PVME concentration profiles in the

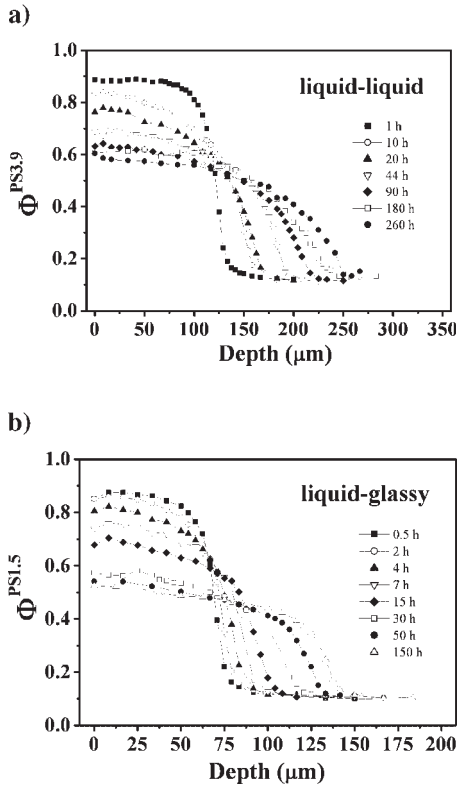


Figure 1. Diffusion profiles of liquid PS in PPO matrices: a) PPO matrix is a highly viscous liquid. The data correspond to the *l*-PS3.9/PPO pair, held at 200 °C for the times indicated in the plot. b) PPO is in the glassy state. The data correspond to one of the *l*-PS1.5/PPO samples held at 160 °C for the times indicated in the legend.

*l*-PVME/PS polymer pair (not shown here). These experiments were performed at temperatures ranging from 15 °C below to 25 °C above the $T_g$ of the polymer matrix (pure PS).

As observed in the plots, the diffusion profiles of the liquid polymer show similar characteristics for experiments performed above and below the matrix $T_g$. At diffusion temperatures slightly above its $T_g$, the high-$T_g$ matrix behaves like a highly viscous liquid during the whole experiment. This case can be thought of as diffusion between a low-viscosity liquid and a highly viscous matrix. The asymmetry observed in the diffusion profiles can be quantitatively explained in terms of the dissimilar mobility between the components of the polymer pair, as discussed in previous work.[4,12] In the experiments conducted at diffusion temperatures below the matrix $T_g$, the matrix remains glassy during the whole process. The asymmetry of the liquid diffusion profiles and the fact that the matrix remains glassy at the temperature of the experiment are concurrent conditions in diffusion mechanisms controlled by mechanical relaxation, and it would be tempting to consider these experiments as examples of Case-II diffusion processes.[5,6]

 

However, our careful analysis of the diffusion kinetics will show that this may not be the case.

We chose two parameters for the investigation of the diffusion kinetics of these liquid polymers: the concentration of liquid polymer at the "plateau" region ($\Phi_{pl}$) and the position of the advancing liquid polymer diffusion front ($z_{df}$), defined as the region on the depth scale where the concentration of liquid polymer drops abruptly. The plateau region coincides with chemical compositions that correspond to the highest polymer mobility and is very sensitive to the features that control the diffusion process. In addition, $\Phi_{pl}$ can be very precisely measured in our experimental setup. In contrast and as discussed above, instrumental artefacts distort the shape of the diffusion front making the precise determination of $z_{df}$ more difficult. We can take advantage of the fact that in systems characterized by diffusion profiles with an almost rectangular-box shape, both parameters are related by the conservation of mass which requires that the product of $\Phi_{pl}z_{df}$ is constant throughout the process.[7b] We obtained the successive positions of the liquid polymer diffusion fronts from this relationship.

Figure 2 shows how the diffusion fronts of the liquid polymers advance into the high-$T_g$ polymer matrices in both *l*-PVME/PS and *l*-PS/PPO systems. The plot includes diffusion experiments conducted at temperatures above and below the matrix $T_g$ (see figure caption). Figure 3 summarizes similar results plotted in Fickean fashion, as functions of the square root of the elapsed diffusion time. In these experiments and differently from previous reports,[5,10] we have taken particular care in examining not only an extended range of diffusion temperatures, but also a wide range of diffusion times. In this way, diffusion data are extended over time scales large enough to make sure whether the evolution is linear or other. From the experimental data shown in Figure 2–3, we can draw some immediate conclusions. a) In both polymer pairs, the liquid diffusion fronts advance more rapidly at higher temperatures. No indication of changes in the diffusion mode when passing through the matrix $T_g$ is observed. b) For all the experiments, the advances of the liquid diffusion fronts toward the (glassy or liquid) matrix are markedly non-linear with time. This fact is not surprising for the experiments conducted at temperatures above the matrix $T_g$ (curve (c) in Figure 2), for which diffusion is presumably Fickean. It does not give support for a Case-II mechanism in experiments conducted at temperatures below the matrix $T_g$, as one of the characteristics of this mechanism is the constant advancing rate of the diffusion front, as a result of the coupling between diffusion and the mechanical relaxation of polymer segments in response to the osmotic-driven swelling stress.[1] c) All the data scale remarkably well with $t^{1/2}$, a typical signature of Fickean diffusion. The slight downward curvature observed in all the experiments at very long diffusion times in Figure 3 is distinctive of liquid-liquid polymer diffusion between components with different $T_g$ and can be quantitatively explained in terms of the changes in the diffusion coefficients as the diffusion process evolves.[4,12]

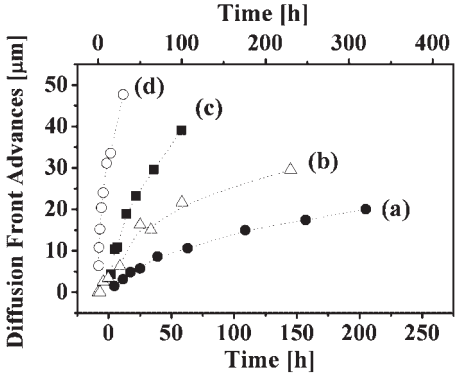


Figure 2. Advances of liquid polymer fronts with increasing diffusion time. The solid symbols and the bottom time axis correspond to *l*-PVME/PS227 held at: (a) 85 °C and (c) 125 °C. The open symbols and the top time axis correspond to *l*-PS1.5/PPO held at: (b) 140 °C and (d) 180 °C.

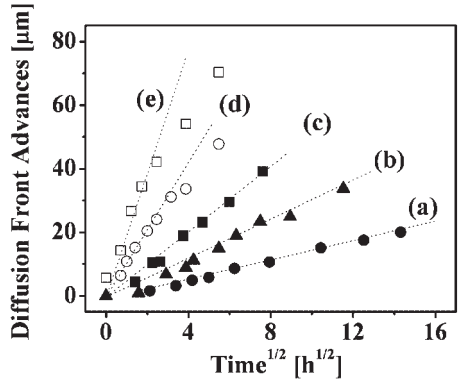


Figure 3. Positions of liquid polymer fronts versus square root of diffusion time. The solid symbols correspond to *l*-PVME/PS227 held at: (a) 85 °C, (b) 105 °C, and (c) 125 °C. The open symbols correspond to *l*-PS1.5/PPO held at: (d) 180 °C and (e) 200 °C.

We now turn our attention to how temperature, and the resulting changes in the physical state of the matrix, operates on the diffusion rates. We examined the changes in the diffusion front velocity ($V_{df}$) in the range of annealing temperatures that encompasses the matrix $T_g$. Figure 4 shows instantaneous values of $V_{df}$, calculated as $dz_{df}/dt$,[b] plotted in Arrhenius fashion for the polymer pairs examined. To focus only on the influence of temperature, we calculated $V_{df}$ data at the same value of liquid polymer concentration at the plateau region ($\Phi_{pl} = 0.7$) and from experiments carried out using similar initial thicknesses for the low-$T_g$ layer (65 μm). The absence of discontinuity in the diffusion behavior when passing through

[b] We calculated instantaneous values for $V_{df}$ following the procedure described in ref.[7a]

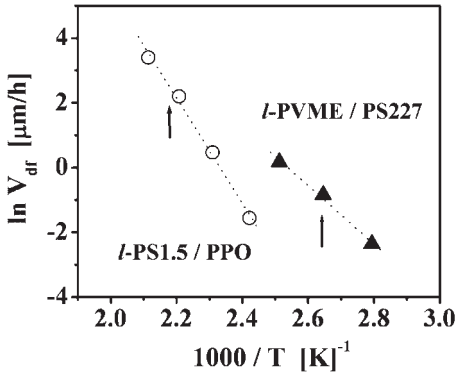


Figure 4. Temperature dependence of instantaneous velocities of the liquid polymer diffusion fronts ($V_{df}$), obtained at $\Phi_{pl} = 0.7$, plotted in Arrhenius form for both *l*-PVME/PS227 and *l*-PS1.5/PPO polymer pairs. The arrows indicate the corresponding glass transition temperature of the amorphous matrix. The dotted lines represent the linear fittings used to calculate the apparent activation energies.

the matrix $T_g$ (arrows in the plot) is remarkable, confirming the observations made on the data shown in Figure 2–3.

The curves yield apparent activation energies ($E_{act}$) of 20 kcal · mol$^{-1}$ for the *l*-PVME/PS pair (range 85–125 °C) and of 36 kcal · mol$^{-1}$ for the *l*-PS/PPO pair (range 140–220 °C). Values of activation energies for viscous flow ($E_{act/v}$) can be obtained from the Williams-Landel-Ferry (WLF) equation, i.e., $E_{act/v} = 2.303RC_1^g C_2^g T^2/(C_2^g + T - T_g)^2$, where $R$ is the gas constant and $C_1^g$ and $C_2^g$ are the WLF parameters calculated at $T_g$ as the reference temperature.[15] These constants, usually obtained from viscoelastic measurements, are well known for the systems studied here.[16,17] The obtained $E_{act}$ values compare well with $E_{act/v}$ corresponding to temperatures well above $T_g$ ($T - T_g = 125$ °C for *l*-PVME/PS227 and $T - T_g = 80$ °C for PS1.5/PPO). This fact suggests that the controlling step of the diffusion process is placed at the liquid polymer-matrix interphase, at liquid polymer concentrations corresponding to a local $T_g$ quite lower than the annealing temperatures. On the contrary, Case II diffusion has been characterized by $E_{act}$ values much higher than those associated with Fickean diffusion, as these correspond to the creep occurring because of the matrix yielding process produced by the osmotic-driven liquid penetration.[1]

## Conclusion

We have shown that the diffusion behavior of the liquid polymers examined here are rather insensitive to the physical state (liquid or glassy) of the high-$T_g$ polymer matrix. Despite the dramatic changes in the relaxation rate of the matrix when going from the liquid to the glassy state (i.e., the change of PS creep rate in the transition range is about three orders of magnitude),[15] no signature of change in the diffusion mode was observed in any of the examined systems. Conversely, the diffusion behavior of the liquid polymer was remarkably continuous when the annealing temperature passed through the matrix $T_g$, with all the characteristics of liquid-liquid polymer diffusion. Typical features of Case-II diffusion, reported in other works as the dominant mechanism in these systems, were not observed here. We may infer that diffusion at these liquid/glassy polymer interphases proceeds similarly and is ruled by the same principles that control the polymer diffusion in the liquid state.

[1] [1a] N. L. Thomas, A. H. Windle, *Polymer* **1980**, *21*, 613; [1b] N. L. Thomas, A. H. Windle, *Polymer* **1981**, *22*, 627; [1c] N. L. Thomas, A. H. Windle, *Polymer* **1982**, *23*, 529.
[2] [2a] C.-Y. Hui, K.-C. Wu, R. C. Lasky, E. J. Kramer, *J. Appl. Phys.* **1987**, *61*, 5129; [2b] C.-Y. Hui, K.-C. Wu, R. C. Lasky, E. J. Kramer, *J. Appl. Phys.* **1987**, *61*, 5137.
[3] [3a] R. C. Lasky, E. J. Kramer, C.-Y. Hui, *Polymer* **1988**, *29*, 673; [3b] T. P. Gall, R. C. Lasky, E. J. Kramer, *Polymer* **1990**, *31*, 1491; [3c] T. P. Gall, E. J. Kramer, *Polymer* **1991**, *32*, 265.
[4] R. J. Composto, E. J. Kramer, *J. Mater. Sci.* **1991**, *26*, 2815.
[5] B. B. Sauer, D. J. Walsh, *Macromolecules* **1991**, *24*, 5948.
[6] E. Jabbari, N. A. Peppas, *Macromolecules* **1993**, *26*, 6229.
[7] [7a] P. F. Nealey, R. E. Cohen, A. S. Argon, *Polymer* **1995**, *36*, 3687; [7b] Q.-Y. Zhou, A. S. Argon, R. E. Cohen, *Polymer* **2001**, *42*, 613.
[8] Y. Feng, R. A. Weiss, A. Karim, C. C. Han, J. F. Anker, H. Kaiser, D. G. Peiffer, *Macromolecules* **1996**, *29*, 3918.
[9] J. P. Tomba, J. M. Carella, D. García, J. M. Pastor, *Macromolecules* **2001**, *34*, 2277.
[10] C. J. Lin, I. F. Tsai, C. M. Yang, M. S. Hsu, Y. C. Ling. *Macromolecules* **2003**, *36*, 2464.
[11] M. Geoghegan, R. A. L. Jones, M. G. D. Van der Grinten, A. S. Clough, *Polymer* **1999**, *40*, 2323.
[12] J. P. Tomba, J. M. Carella, D. García, J. M. Pastor, *Macromolecules* **2004**, *37*, 4940.
[13] J. P. Tomba, J. M. Carella, J. M. Pastor, J. C. Merino, *Polymer* **2002**, *43*, 6751.
[14] J. P. Tomba, E. de la Puente, J. M. Pastor, *J. Polym. Sci., Part B: Polym. Phys.* **2000**, *38*, 1013.
[15] J. D. Ferry, "*Viscoelastic Properties of Polymers*", Wiley, New York 1980.
[16] [16a] R. J. Composto, E. J. Kramer, D. M. White, *Polymer* **1990**, *31*, 2320; [16b] W. M. Prest, R. S. Porter, *J. Polym. Sci., Part A: Polym. Chem.* **1972**, *10*, 1639.
[17] [17a] P. F. Green, D. B. Adolf, L. Gilliom, *Macromolecules* **1991**, *24*, 3377; [17b] A. Ajji, L. Choplin, R. E. Prudhomme, *J. Polym. Sci., Part B: Polym. Phys.* **1988**, *26*, 2279; [17c] R. Stadler, L. de L. Freitas, V. Krieger, S. Klotz, *Polymer* **1988**, *29*, 1643.

 